Engineering and Technology Journal 41 (01) (2023) 142-150

Engineering and Technology Journal
Journal homepage: https://etj.uotechnology.edu.iq

Determination of Impingement Cooling Fluid Temperature-Time Profile for Extracted Tiger-Nut Juice (Cyperus Esculentus) by Lumped Thermal Mass Analysis

N.M. Azubuike[a]*, Onah Thomas Okechukwu[b], Egwuagu Michael Onyekachi[b]

[a] Department of Mechanical Engineering, Caritas University, Amorji-Nike Enugu Enugu state Nigeria,

[b] Department of Mechanical and Production Engineering, Enugu State University of Science and Technology, Enugu, Enugu State Nigeria
*Corresponding author Email: zubbymike@gmail.com

HIGHLIGHTS

- Tiger-Nut juice extracted for impingement
- Tiger-Nut juice extracted for impingement process on a run-out table for steel production, a novel impingement fluid.
- The use of Lumped thermal mass analysis makes it less cumbersome than pool boiling mechanism analysis to determine the cooling rate.

ARTICLE INFO

Handling editor: Sattar Aljabair

Keywords:
Impingement gaps; lumped thermal-mass-Analysis; Run-out table; Tiger-Nut Juice; Temperature Time Profile.

ABSTRACT

Determination of Temperature-Time Profile by the Lumped thermal mass analysis (LTMA) method using Tiger-Nut Juice as the impinging fluid on the cooling system was carried out. With a stationary hot steel plate on a modified run-out table for the top surface controlled the accelerated cooling process. This was evaluated with pipe diameters of 10 mm, 15 mm, 30 mm, 35 mm, and 40 mm by single jet Tiger-Nut Juice impinging fluid, impingement gaps of 115 mm, 125 mm, 135 mm, 145 mm, and 155 mm, initial surface temperatures from 450°C – 410°C and at sub-cooled temperatures from 150°C–110°C. The analysis reveals a faster cooling rate for both diameters at an impingement gap of 155 mm. Diameter 10mm with 1.8°C/sec average rate, for impingement gap of 115 mm, 1.8°C/sec for impingement gaps of 125 mm, 135 mm and 145 mm and 1.9°C for 155mm. This optimal temperature-time profile of Tiger Nut Juice impingement cooling infers that a higher cooling rate is achieved using smaller pipe diameter D and higher impingement gap H. In addition, it showed evidence of less Leiden frost phenomenon; hence, extracted tiger nut juice fluid can perfectly serve as a substitute for water at smaller pipe diameters and higher impingement gaps. Also, it was inferred that it also cools at a bigger pipe diameter with a lower impingement gap.

1. Introduction

Recently, with the continual enhancement of steel material functions, such as higher strength and better ductility, the growing demand for cost-cutting by reducing the use of alloying elements and streamlining processes: the thermo-mechanical control process (TMCP) has become increasingly important, as discoursed by Kazuaki, Kumar, and Maharshi, [1, 2, and 3]. Steel and other alloys have many applications in engineering practice under many conditions, requiring that the steel have several properties for various applications, as revealed by Alqash and Nwankwo [4and 5]. At one point of the designer's desired need of operations, steel materials are subject to either of the following: bending and, at the other, twisting. As tool materials that will cut others, they may require hardness and toughness with no brittle cutting edge, and they may as well be able to withstand various stresses. Serving under these conditions and more, they require certain specific properties to be able to withstand the various conditions the designers subject them to, as agreed by Antonio, Onah, and Onah [6, 7, and 8]. Meanwhile, some materials may be fully or partially lacking in these specifics. These lacks or deficiencies are fulfilled before now through the process of heat treatment, which is not cost-effective. Therefore, there is a need for improving steel properties, which demands reducing the cost of alloying elements and streamlining processes. Hence, need for a better process in steel production that provides for heating and control cooling, as suggested and agreed upon by Kazuaki and Onah [1,9].

The improved design ROT discoursed by Onah and Nwankwo [9, 10] was for top surface stationary only. Mechanistic modeling of pool boiling has existed and is cumbersome to analyze. Hence the need for a simpler analysis model – lumped thermal mass analysis, for evaluating the temperature-time profile for Tiger-Nut Juice as impinging fluid.

http://doi.org/10.30684/etj.2022.134483.1239
Received 27 June 2022; Accepted 27 August 2022; Available online 03 October 2022
2412-0758/University of Technology-Iraq, Baghdad, Iraq
This is an open access article under the CC BY 4.0 license http://creativecommons.org/licenses/by/4.0

Over the years in steel production, water has been a major impingement fluid, from time of alloying to heat treatment to controlled rolling of steel, until the accelerated controlled cooling era came to accommodate the use of many fluids. Nwankwo [5] discoursed that it opens up the thermo-mechanical controlled process where accelerated controlled cooling is part, and jet impingement cooling is part of accelerated controlled cooling. Hence, the use of many fluids for cooling emerged.

Noel [11], the novelty in their work was the introduction of a new fluid for jet impingement cooling – automatic transmission fluid. Using numerical simulation, they studied heat transfer performance for a novel rotating liquid jet impingement cooling system. Their study consists of a rotational pipe with two nozzles. The target is a cylindrical ring, which contains curved target surfaces. They showed the effect of pipe rotation on heat transfer performance and compared existing literature regarding jet impingement cooling systems.

Mistutakee et al. [12] studied the cooling system of boiling heat transfer on a hot steel plate cooled by an inclined circular bottom surface using water. They focused on the inclined angle at the bottom of the hot steel plate and the flow rate effect on heat extraction. He varied the flow rate, ROT speed, and inclined angles from 35 -55l/min, 0 -1 m/s, and 10-30ºC, respectively. With these variables, he employed the inverse heat conduction model and his measurements and calculated the boiling curve or heat fluxes as a function of plate surface temperature.

Avadhash et al. [13] began by acknowledging the superiority of jet impingement cooling as always preferred over the other cooling methods due to its high heat removal capability. Their experiment was on the rewetting behavior of a hot horizontal downward facing hot surface by mist jet impingement. Mist jet impingement cooling offers an alternative method to uncontrolled rapid cooling, particularly in the steel and electronics industries. The dispersal of water droplets into an airflow can be characterized as either spray cooling or mist jet cooling. In spray cooling, compressed water is atomized by pressure at the nozzle, while in mist cooling; droplets are atomized by compressed air. Mist jets thus allow smaller droplets.

Figure1 shows the schematic of free surface jet impingement and profile model of single jet surface planar jet hydrodynamics used for this study. This shows the stagnation and wetted areas'

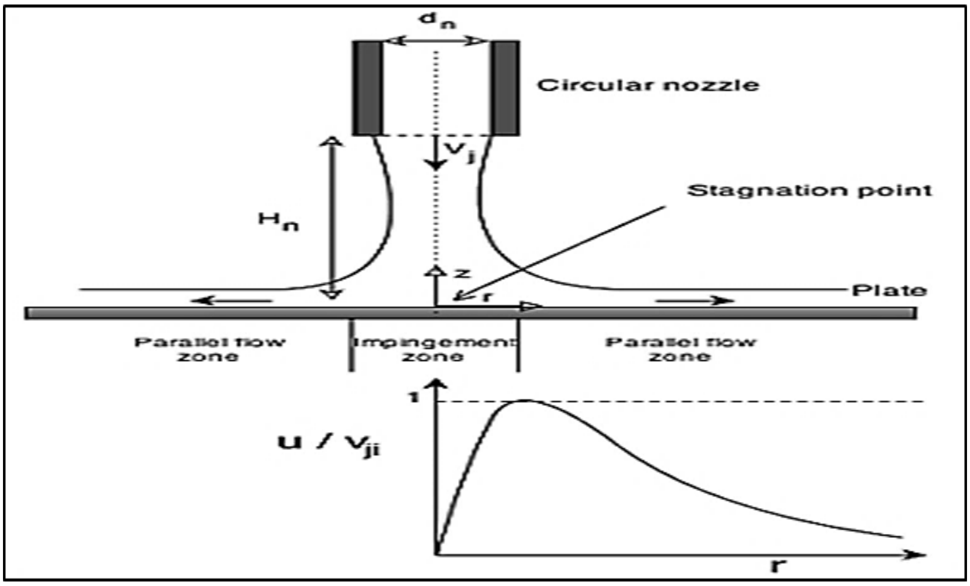

Figure 1: Schematic of free surface jet impingement and profile of Single Jet surface planar jets, Jeffery [14]

Singh and Maharshi [15, 3] applied the air impingement cooling process in the food industry. They affirmed that the surface heat transfer coefficient in impingement cooling depends upon several impingement parameters, namely nozzle design, the geometry of the object being cooled, jet exit to object distance, the velocity of the air jet, and jet confinement. The effects of these impingement parameters on the distribution of local surface heat transfer coefficient on a cylindrical object were studied in a steady and unsteady state. Numerical model solution solved using CFD and validated by experiments (using PIV) to optimize these parameters. Heat transfer maximum found at H/D of 3. They concluded that data from their work could be used to design and optimize an impingement system for a given set of conditions. Hence, used to determine the power requirement

QI and Onah [16, 7] experimented with quenching stainless steel using a single jet oil impingement cooling process on the bottom surface of the plate. They heated the sample specimen from 100℃ to 900℃, and their objective was to know the effect of oil as an impingement fluid on the bottom surface. Their varying parameters were 113 to 381 ml/min, 3.1 to 12 psi oil pressure, and impingement height of 0.6 to 1 cm. Test results also show that oil heat transfer coefficient and heat flux keep increasing as plate temperature increases.

In all the literature, water has been dominant, and few others are mentioned as impinging fluid. The Leidenfrost phenomenon affects water Gilles and Md Lokman [17,18]. Pool boiling analysis has predominantly been the analytical model for the temperature-time plot. This analytical method has been cumbersome for engineers, as stated in their various works by Onah and Gilles [9,17]. Therefore, this present study seeks to use extracted Tiger-Nut juice as impinging fluid and lumped thermal mass analysis as an analytical method for plotting temperature-time. Tiger-Nut juice is expected to have less Leiden frost phenomenon, and lumped thermal mass analysis is less cumbersome and time-consuming.

2. Methodology

Figure 2 shows a schematic diagram of a pilot scale modified run-out table (ROT) facility having the capacity for top and bottom surface cooling, installed at Metallurgical and Material Engineering Laboratory (MMEL), Enugu State University of Science and Technology (ESUT)

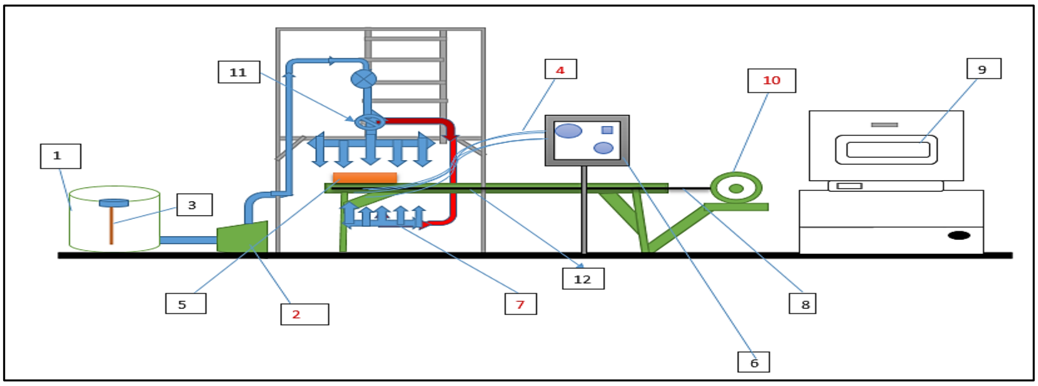

Figure 2: Schematics of the Modified ROT set-up plant: 1. Water tank, 2. Electric pump, 3.Heater, 4. Thermocouple wires, 5. The workpiece and its carrier, 6.Thermocouple control panel, Workpiece bed, 7. Bottom Impingement nozzle, 8. Motorized screw conveyor, 9. Furnace, 10. Electric motor, 11. Flow valve, 12. Flow meter, 13. Ladder, 14. Furnace support, 15, PVC Pipes, 16. Pressure gauge

The plant houses the combination of various parts aforementioned. The experiment features the cooling system – a closed loop where the volume of used water was 1.56 $m^{3,}$ circulated throughout the system. Initial temperature, water temperature, impingement height, and flow rate were varied and controlled. The system stabilized before the sample hot plate was placed under the headers. Four thermocouples were read out using the mounted control panel for the temperature and average taken.

Tiger nut (Cyperus Esculentus), seeds of 15 kg of tiger nut seeds were purchased from Orie market Emene Enugu Nigeria, this was blended without the addition of water, and the juice was extracted with a sieve. As a result, 5liters of tiger-nut juice was produced through the process and was used as Tiger-Nut Juice jet impingement cooling for the experiment.

Table 1 shows the physical properties of the sampled impinging fluid – tiger-nut extracted juice. These properties are obtained at 50 to 60 degrees Celsius''

Table 1: Properties of Sampled Fluid Usman, [19]

Properties Of Tiger-Nut Juice						
S/N	**Fluids**	**Density(Kg/M^3)**	**Viscosity (Kg/M-S)**	**Thermal Conduct W/Mk**	**Specific Heat J/Kgk**	**Temp ℃**
1	Tnj-Jic	705	$1.15x10^{-1}$	0.133	1875	50- 60

2.1 Lumped Thermal Mass Model Analysis for Heat Transfer Coefficient H

The basic concept in the analysis of the lumped thermal mass model is that the body's interior temperature remains constant at all times during a heat transfer process. This is because the temperature of such a body is the only function of time, T = T(t). This also means that in analysis, no temperature gradient exists -which means that the body's internal resistance (conduction) is negligible compared to external resistance (convection). In this model, when mass, a well-conducting solid or a well-mixed fluid, is subjected to heating or cooling by exposure to an environment with which it exchanges heat. One assumes that temperature variations within the mass can be neglected compared to the temperature difference of mass and surrounding fluids, Shankar [20].

The control volume of the lumped thermal mass model of the impingement process in Figure 3 simplifies the complicated modeling process of impingement cooling, which involves conduction and convection. In this process, we assumed that:

1) Heat transfer from a hot steel plate is seen as a lumped mass.
2) The mass resistance heat transfer is negligible when compared with resistant heat transfer with the impinging fluid.
3) The volume of mass remains unchanged.

The 2-D surface cooling heat transfer deals with a thickness of 12 mm and a length of 230 mm with a width of 120mm.

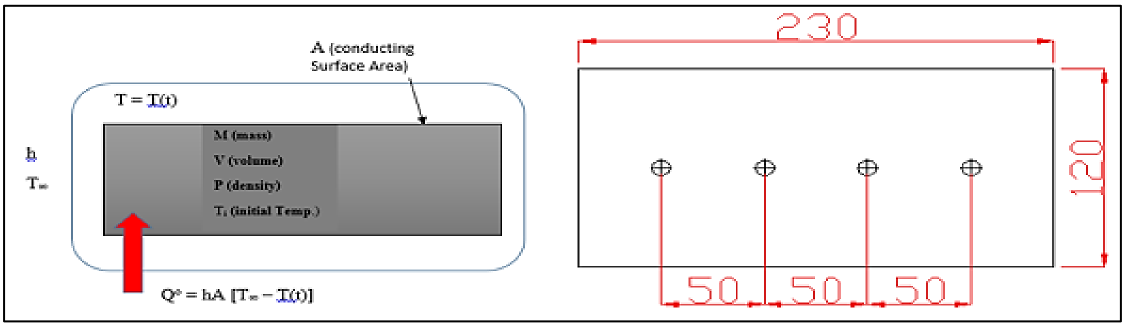

Figure 3: Control volume of lumped thermal mass model Analysis of impingement process

The lumped mass method is based on the control volume of the steel plate shown in Figure 3. The mass behaves as a single lump of temperature, T. Thus equating heat transfer conduction at the bottom to that conducted at the top by convection since boiling heat is infinitesimal and was collapsed into convection, in Equation 2 as Shankar [20].

$$MC\frac{d}{dt}(T_S - T_\infty) = -hA(T_S - T_\infty) \tag{1}$$

$$\frac{\partial(T_S - T_\infty)}{(T_S - T_\infty)} = \frac{-hAdt}{mcp} \tag{2}$$

By integration,

$$\int_{t=0}^{t} \frac{d(T-T_\infty)}{T-T_\infty} = Log_e\left(\frac{T-T_\infty}{T_S-T_\infty}\right) t = 0, = \frac{-hAt}{mcp} \tag{3}$$

$$\text{Thus, } Log_\theta = \frac{-hAt}{mcp} \tag{4}$$

The gradient is given in Equation 6, as,

$$\text{gradient is } -\propto = \frac{-hAt}{mcp} \tag{5}$$

$$\text{From which, } h = \propto \rho w c p \tag{6}$$

Where h is convective heat transfer coefficient W/m^{2}k, t is the time in seconds, T is the initial temperature, m is the mass of the sample in kg, A is the area of the specimen in m^2, T $_s$ is the surface temperature and the T_∞ is the infinite temperature.

$$for\ steel, density\ \ \rho = \frac{7900hg}{m^3},\ specific\ heat\ Cp = \frac{500J}{kgk};\ sampled\ thickness\ w = 0.012m, \propto$$

, is a gradient from equation (7)

3. Results and Discussion

The results below are the experimental values of constant pipe diameters D with variant impingement gaps H corresponding initial surface temperatures T_s control cooled at constant sub-cooled temperatures T_{sub}.

Table 2 shows the initial surface temperature T_s of 450, 440, 430, 420, and 410ºC on sampled steel and the time t(s), variant impingement gaps H of 115, 125, 135, 145, and 155 mm at constant pipe diameter D=10 mm. Controlled subcooled temperature T_{sub} of 150ºC

Table 2: 150oC @D=10mm Variant T and H

T=450 @D=10mm(H=115)		T=440 @D=10mm(H=125)		T=430 @D=10mm(H=135)		T=420 @D=10mm(H=145)		T=410 @D=10mm(H=155)	
t(s)	Ts	t(s)	Ts	t(s)	Ts	t(s)	Ts	t(s)	Ts
0	450	0	440	0	430	0	420	0	410
42.5	400	41.5	391.67	40	383.34	38.12	375	36.21	366.67
85	350	83	343.34	80	336.68	76.24	330	72.42	323.34
127.5	300	124.5	295.01	120	290.02	114.36	285	108.63	280.01
170	250	166	246.68	160	243.36	152.48	240	144.84	236.68
212.5	200	207.5	198.35	200	196.7	190.6	195	181.05	193.35
255	150	249	150	240	150	228.72	150	217.26	150

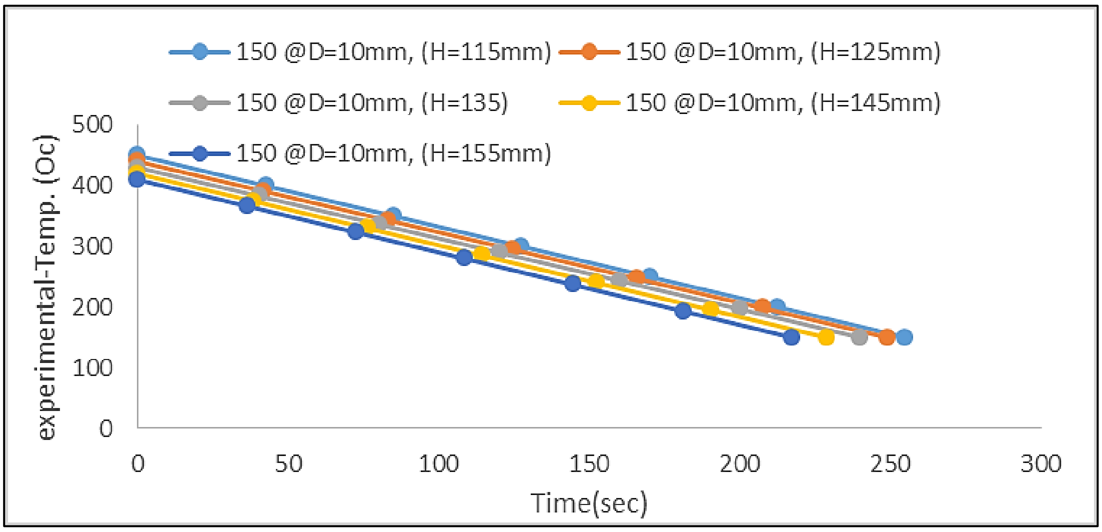

Figure 4: Temperature-time Cooling Profile @ 150ºC for D=10 mm and H=115, 125, 135, 145 and 155 mm

Figure 4, Depicts the temperature-time controlled cooling profile for a diameter of 10 mm and varied impingement gaps of 115 mm, 125 mm, 135 mm, 145 mm, and 155 mm. From the straightness of the plot, the cooling rate was highest at starting top surface that has the highest temperature, followed by the middle and down to the bottom surface. The plot is for the same diameter D=10mm and the same controlled subcooled temperature T_{sub} =150ºC, but with varied impingement height H of 115mm, 125mm, 135mm, 14mm, and 155mm. The impingement gap of 155mm cooling rate showed a higher value than the impingement gap of 115 mm. At 115 mm it shows rate of 1.8ºC/sec and 1.8ºC/sec for 125 mm, 135 mm, 145 mm, while 155 mm showed 1.9ºC/sec. Impinging with tiger-nut fluid, better steel cooling is achieved with a smaller pipe diameter D and corresponding higher impingement gap H, also studied with water by Onah and Onah [21, 22]. Table 3 shows the same initial surface temperature T_s, time t(s), and impingement gaps but a subcooled temperature of 140ºC for a diameter of 15 mm.

Table 3: 140°C @D=15 mm Variant T and H

T=450 @D=15mm(H=115)		T=440 @D=15mm(H=125)		T=430 @D=15mm(H=135)		T=420 @D=15mm(H=145)		T=410 @D=15mm(H=155)	
t(s)	**Ts**	**t(s)**	**Ts**	**t(s)**	**Ts**	**t(s)**	**Ts**	**t(s)**	**Ts**
0	450	0	440	0	430	0	420	0	410
42.5	398.34	41.5	390	40	381.67	36.19	373.34	37.09	350
85	346.68	83	340	80	333.34	72.38	326.68	74.18	305.7
127.5	295.02	124.5	290	120	285.01	108.57	289.02	111.27	245.1
170	243.36	166	240	160	236.68	144.76	233.36	148.36	190.9
212.5	191.7	207.5	190	200	188.35	180.95	186.7	185.45	160
255	140	249	140	240	140	217.14	150	222.54	140

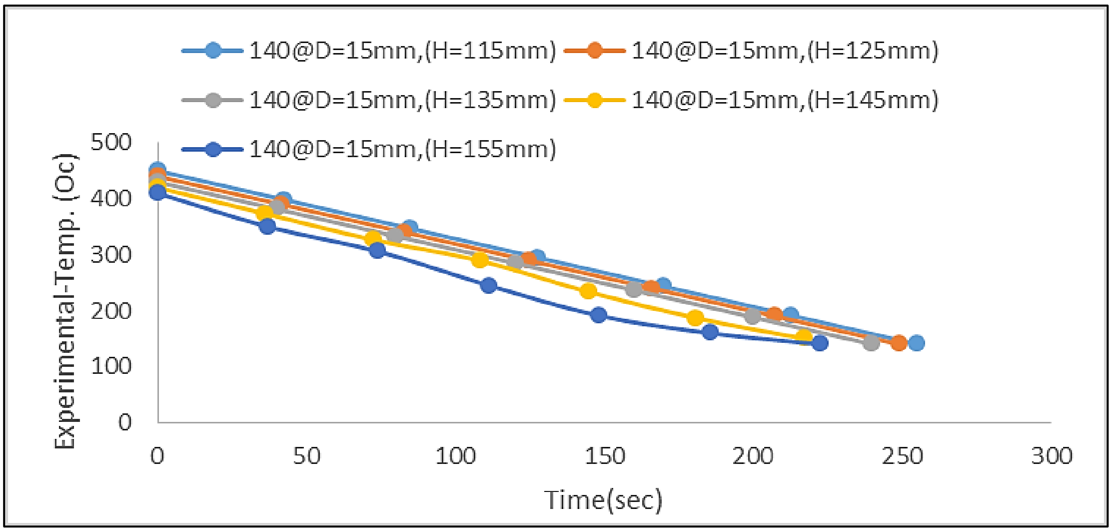

Figure 5: Temperature-time Cooling Profile @ 140°C for D=15 mm and H=115, 125, 135, 145 and 155 mm

Figure 5, Shows a temperature-time controlled cooling profile for a diameter of 15mm with the same varied impingement gaps sub-cooled to 140°C. The plot pattern is the same as in diameter of 10 mm. Impingement gaps 115, 125, and 135 mm showed a cooling rate of 1.8°C/sec, while 145 mm and 155 mm showed 1.9°C/sec. Again, this depicts that for tiger nut fluid, a better cooling rate is achieved with smaller pipe diameter D and a higher impingement gap H, as revealed by Purna and Kumar's work [23, 2].

Table 4 also shows the same initial surface temperature T_s, same impingement gaps H and time t(s), but a subcooled temperature of 130°C for a diameter of 30 mm.

Table 4: 130℃ @D=30 mm Variant T and H

T=450 @D=30mm(H=115)		T=440 @D=30mm(H=125)		T=430 @D=30mm(H=135)		T=420 @D=30mm(H=145)		T=410 @D=30mm(H=155)	
t(s)	**Ts**	**t(s)**	**Ts**	**t(s)**	**Ts**	**t(s)**	**Ts**	**t(s)**	**Ts**
0	450	0	440	0	430	0	420	0	410
42.5	396.67	41.5	388.34	40	380	37.09	371.67	36.19	363.34
85	343.34	83	336.68	80	330	74.18	323.34	72.38	316.68
127.5	290.01	124.5	286.02	120	280	111.27	275.04	108.57	270.02
170	236.68	166	233.36	160	230	148.36	226.74	144.76	223.36
212.5	183.35	207.5	181.7	200	180	185.45	178.41	180.95	176.7
255	130	249	130	240	130	222.54	130	217.14	130

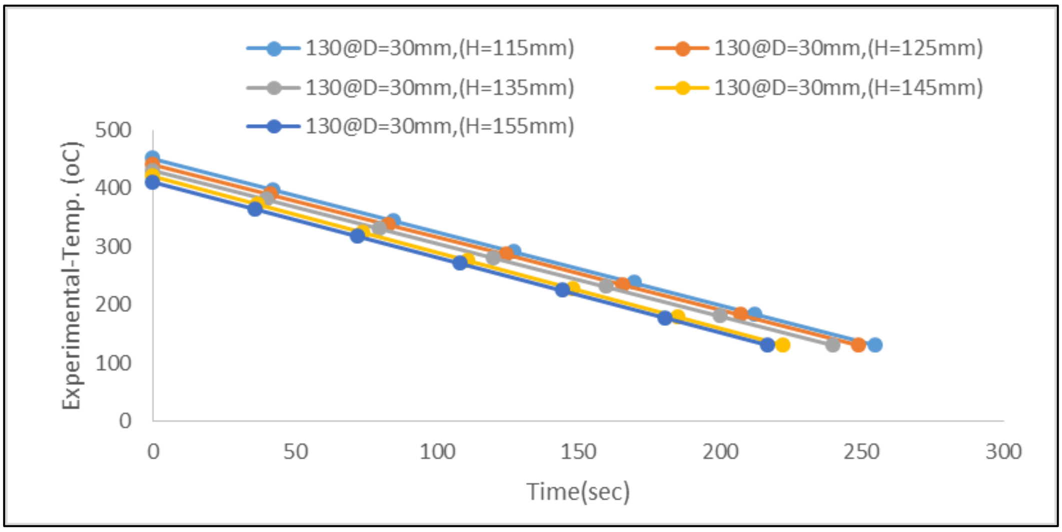

Figure 6: Temperature-time Cooling Profile @ 130°C for D=30 mm and H=115, 125, 135, 145 and 155 mm

Figure 6 Displays the temperature-time controlled cooling profile for a diameter of 30 mm with the same varied impingement gaps but controlled subcooled temperature of 130℃. Again the plot maintained the same temperature gradient pattern. The cooling rate shows an impingement gap of 115 mm at 1.8℃/s while the rest have 1.9°c/s. However, it maintained that a better cooling rate for austempering of a hot steel plate is attainable at a higher impingement gap.

Table 5 shows the same initial surface temperature Ts and impingement gaps H and time t(s), but subcooled to 120℃ for a diameter of 35 mm.

Table 5: 120℃ @D=35 mm Variant T and H

T=450 @D=35mm(H=115)		T=440 @D=35mm(H=125)		T=430 @D=35mm(H=135)		T=420 @D=35mm(H=145)		T=410 @D=35mm(H=155)	
t(s)	**Ts**	**t(s)**	**Ts**	**t(s)**	**Ts**	**t(s)**	**Ts**	**t(s)**	**Ts**
0	450	0	440	0	430	0	420	0	410
43	395	42.5	386.67	41.5	378.34	40	370	37.09	361.67
86	340	85	333.34	83	326.68	80	320	74.18	313.34
129	285	127.5	280.01	124.5	275.02	120	270	111.27	265.01
172	230	170	226.68	166	223.36	160	220	148.36	216.68
215	175	212.5	173.35	207.5	171.7	200	170	185.45	168.35
285	120	255	120	249	120	240	120	222.54	120

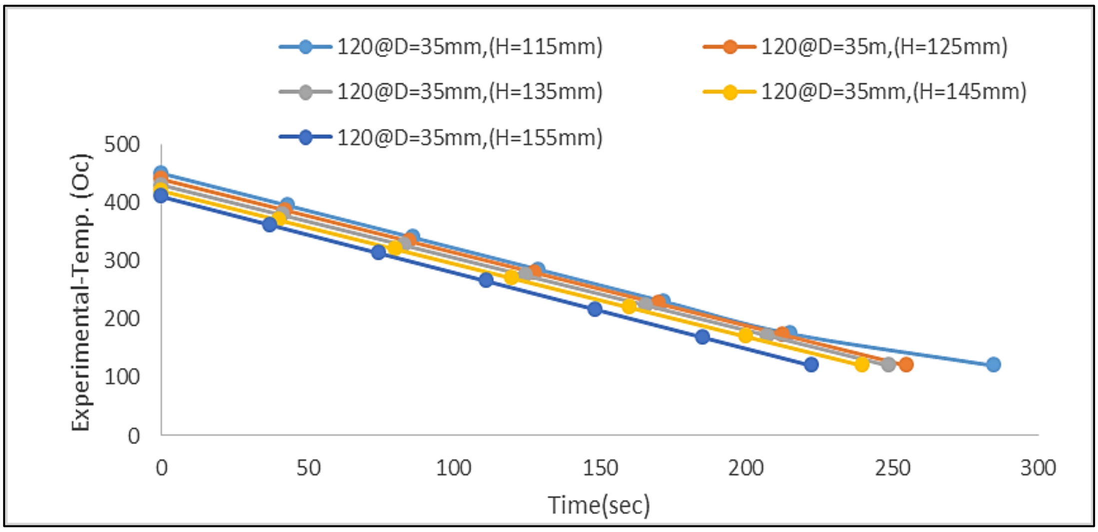

Figure 7: Temperature-time Cooling Profile @ 120°C for D=35 mm and H=115, 125, 135, 145 and 155 mm

Figure7 shows the temperature-time controlled cooling profile for a diameter of 35 mm with the same varied impingement gaps and sub cooled to a controlled temperature of 120°C, maintaining the same pattern as others. The cooling rate began to drift from what is maintained at the other diameters. For example, an impingement gap of 115 mm shows a cooling rate of 1.6°C/s, and gaps of 125 mm and 135 mm show the same cooling rate of 1.7°C/s and 1.8°C/s cooling rate for gaps of 145 mm and 155mm. Following this drifting, we inferred that a bigger pipe diameter with a lower impingement gap would achieve a better cooling rate.

Table 6, Shows the initial surface temperature T_s, impingement gaps H as others, and time t(s) for a sub cooled temperature of 110°C with a diameter of 40mm.

Table 6: 110°C @D=40 mm Variant T and H

T=450 @D=40mm(H=115)		T=440 @D=40mm(H=125)		T=430 @D=40mm(H=135)		T=420 @D=40mm(H=145)		T=410 @D=40mm(H=155)	
t(s)	Ts	t(s)	Ts	t(s)	Ts	t(s)	Ts	t(s)	Ts
0	450	0	440	0	430	0	420	0	410
47	393.34	43	385	42.5	376.67	41.5	368.34	40	360
94	336.68	86	330	85	323.34	83	316.68	80	310
141	280.02	129	275	127.5	270.01	124.5	265.02	120	260
188	223.36	172	220	170	216.68	166	213.36	160	210
235	166.7	215	165	212.5	163.35	207.5	161.7	200	160
282	110	285	110	255	110	249	110	240	110

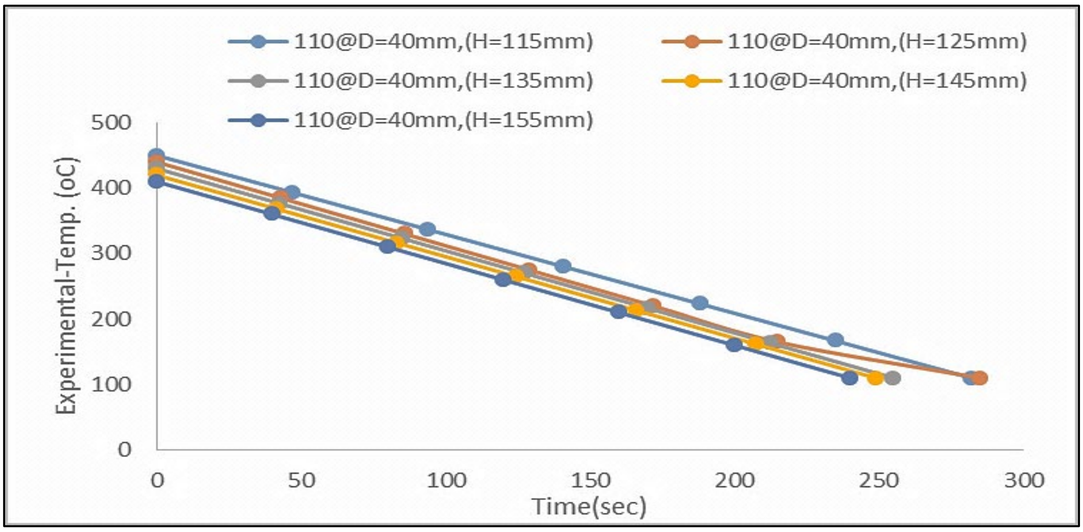

Figure 8: Temperature-time Cooling Profile @ 110°C for D=40 mm and H=115, 125, 135, 145 and 155 mm

Figure 8, Displays the temperature-time controlled cooling profile for the diameter of 40mm with the same varied impingement gaps and sub cooled to a controlled temperature of 110°C. From the cooling rate, the drifting continued with a gap of 115 mm, having 1.6°C/s and 1.5°C/s for 125 mm, with gaps of 135 mm, 145 mm, and 155mm, showing 1.7°C/s. It is suggestive that increasing the pipe diameter D with a lower impingement gap H would give a better cooling rate using tiger-nut extracted juice as impingement fluid for steel au tempering that gives the designer's desired microstructure.

4. Conclusions

The experimental analysis of the jet impingement cooling process, using Tiger-Nut juice as impinging fluid in place of water and lumped thermal mass analysis in place of pool boiling mechanism for the model, was carried out in a modified run-out table. Variant nozzle diameters D, impingement gaps H, surface temperatures $T_{s,}$ and sub cooled controlled temperatures T_{sub} generated the data for the temperature-time plot. The temperature-time plot of Tiger-nut Juice impingement cooling fluid showed the same cooling pattern as water impingement cooling, as shown by Singh and Jay [15, 24].

The analysis showed a cooling rate from 1.5°C/s to 2.0°C/s for the diameters and all impingement gaps. Thus, the results revealed that smaller diameters with higher impingement gap are required for better steel cooling, and bigger diameter requires shorter impingement gap for better au tempering of steel plates.

However, based on submission, the cooling rate achieved using smaller pipe diameters D and higher impingement gaps H suggests a better rate than the 0.2°C/s - 0.3°C/s by Singh [15]. Furthermore, it suggests that cooling steel with a bigger pipe diameter requires shorter impingement gaps for better microstructural properties, as evident in the shifting of the cooling rate. These results showed Tiger-Nut a good impingement fluid that can substitute for water

Author contribution

All authors contributed equally to this work.

Funding

This research received no specific grant from any funding agency in the public, commercial, or not-for-profit sectors.

Data availability statement

The data that support the findings of this study are available on request from the corresponding author.

Conflicts of interest

The authors declare that there is no conflict of interest.

References

[1] Kazuaki et al, Water quenching cfd (computational fluid dynamics) simulation with cylindrical impinging jets, in Nippon stall and sumitomo metal technical report, 2016.

[2] A. A. Kumar, numerical study of inclined air jet impingement cooling of a cylinder, in international conference on computational methods for thermal problems, 2018.

[3] Maharshi, computational modeling of liquid jet impingement onto heated surface, Ph.D. Thesis to Darmstadt, 2017.

[4] S. I. Alqash, numerical simulations of hydrodynamics of multiple water jet impinging over a horizontal moving plate, in numerical simulations of hydrodynamics of multiple water jet impinging over a horizontal moving plate, vancouver, university of British Columbia, Thesis/Dissertation, 2015. Jd1101777. https://doi.org/10.14288/1.0166718

[5] Nwankwo, et al, application of jet impingement cooling in steel production: a review of constrains and prospects, Int. J. Mech. Prod. Eng. Res. Dev., 12 (2022) 1-8.

[6] Antonio Gorni and José Herbert Dolabela Da Silveira, accelerated cooling of steel plates: the time has come, J. ASTM Int. 5 (2014) 8 – 15. https://doi.org/10.1520/JAI101777

[7] T.O. Onah, a. M. nwankwo, And b. U. ugwuanyi, steel influence of controlled water jet impingement cooling on mechanical and metallurgical properties of hot-rolled plates, Explorematics J. Innov. Eng. Technol., 3 (2019), 14 – 22.

[8] T. O. Onah, j. C. edeh, b. N. nwankwojike, development and comparative evaluation of controlled water jet impingement cooling system for hot-rolled steel plates by mechanical and metallurgical assessments, Int. J. Mech. Prod. Eng. Res. Dev., 11 (2021) 147 – 164.

[9] T. O. Onah, A. O. Odukawe, S. O. Egbuna, parametric analysis of impingement gaps on hot steel plate cooling by water jet, international digital organization for scientific research idosr journal of science and technology, 3 (2018) 18 – 32.

[10] A. M. Nwankwo, et al. Analysis of existing temperature-time profile of jet impingement cooling system for steel production, Am. j. Eng. Res., 11 (2022) 113 -120.

[11] L. C. Noel, a study of boiling heat transfer on a hot stell plate cooled by inclined circular bottom water jet; M.Sc. Thesis on material engineering, university of British Columbia, 2006.

[12] Mitsutakee et al, heat transfer during transient cooling of high temperature surface with impingement jet, Int. J. Heat Mass Transfer, 37 (2001) 321 – 330. https://doi.org/10.1007/5002310000141

[13] A. K. Sharma, S. K. Sahu, an experimental study on heat transfer and rewetting behavior of hot horizontal downward facing hot surface by mist jet impingement, j. App. Therm. Energy, 151 (2019) 459-474. https://doi.org/10.1016/j.applthermaleng.2019.02.038

[14] A. Jeffery advanced engineering mathematics, academic press, 2011.

[15] S. K. Singh ,R. Paul Singh, air impingement cooling of cylindrical object using slot jets, 2019. https://doi.org/10.1007/978-0-387-75430-7_5

[16] Qi et al, heat transfer by a rotating liquid jet impingement cooling system, in proceedings of the as me, international mechanical engineering congress and exposition, india, 2018. https://doi.org/10.1115/imece2018-88377

[17] G. A. V. P. Gilles, modeling of transient bottom jet impingement boiling, Int. j. Heat Mass Trans., 136 (2019) 1160-1170. https://doi.org/10.1016/j.ijheatmasstransfer.2019.03.060

[18] Md lokman and rebei bel, f. A., multi-jet impingement cooling of a hot flat steel plate, in international conference on applied energy, sweden, 2014. https://doi.org/10.1016/j.egypro.2014.12.224

[19] E. A. Usman et al., Effect of moisture content variation on thermo-physical properties of brown variety tigernut(peruse esculent us), Arise Zone J. Eng. Technol. Environ., 15 (2019) 714-724.

[20] R. S. Shankar, unsteady heat transfer: lumped thermal capacity model, Clarkson University, 2019.

[21] T. O. Onah, odukwe, a. O. And ojobor, s. N., Effect of impingement heights on temperature time cooling curve on a run-out table system, Int. J. Multidiscip. Res. Dev., 4 (2017) 97 – 105.

[22] Onah, et al, evaluation of temperature profile on pool boiling using jet jet impingement cooling system, Am. J. Eng. Res., 7 (2018) 304-310.

[23] c. M. Purna, model based numerical state feedback control jet impingement cooling of a steel plate by pole placement technique., Int. J. Comput. Eng. Res. , 3 (2013) 2205-2215. https://doi.org/10.1080/10407782.2013.772869

[24] J .M .Jhaet .al, jet impingement cooling of a hot moving steel plate: an experimental study, J. Therm. Energy Gener. Trans. Storage, Convers. , 29 (2016) 1-17. https://doi.org/10.1080/08916152.2015.1046019